Modulating Optical Properties of Graphene Oxide: Role of Prominent Functional Groups

Priya Johari* **and Vivek B. Shenoy***

School of Engineering, Brown University, Providence, Rhode Island 02912, United States

ABSTRACT To modulate the electronic and optical properties of graphene oxide *via* controlled deoxidation, a proper understanding of the role of the individual functional group in determining these properties is required. We, therefore, have performed *ab initio* density functional theory based calculations to study the electronic and optical properties of model structures of graphene oxide with different coverages and compositions. In particular, we considered various concentrations of major functional groups like epoxides, hydroxyls, and carbonyls, which mainly consititute the graphene oxide and the reduced graphene oxide. Our calculated electron energy loss spectra (EELS) demonstrate the π plasmon peak to be less sensitive, while $\pi + \sigma$ plasmon is found to have a significant blue shift of about 1.0−3.0 eV, when the concentration of epoxy and hydroxyl functional groups in graphene oxide vary from 25% to 75%. However, the increase in carbonyl groups in the center of the graphene sheet creates holes, which lead to the red shift of the EELS. In the case of 37.5% of oxygen-to-carbon ratio, we find the π plasmon peak to be shifted by roughly 1.0 eV as compared to that of the pristine graphene. Our results agree well with the experimental findings which suggest a blue shift in the EELS of graphene oxide and an absorption feature due to a π electron transition of the carbonyl groups at a lower energy than that of epoxy and hydroxyl groups. We also show that the increase in the width of the hole created by the carbonyl groups significantly decreases the optical gap and opens the band gap, and thus, we argue that reduced graphene oxide with mostly carbonyl groups could be a useful material for developing tunable opto-electronic nanodevices.

KEYWORDS: two-dimensional materials · graphene oxide · density functional theory · EELS · plasmon

Since the discovery of graphene, numerous researchers have been involved in exploring its remarkable properties and wide range of applications. This two-dimensional material, which is just an atom thick, has interesting electronic, thermal, optical, and mechanical properties;[1,2] however, its band gap of zero restricts it to device application in nanoelectronics.[3] A gap can be introduced in graphene sheets either by nanopatterning[4,5] or by chemical treatment.[6−8] The latter has a greater advantage because of the ease to scale up production.[9] Graphene oxide (GO), an example of chemically treated graphene, has most recently emerged as a potential alternative to graphene. Adsorption of oxygen in the form of epoxy, hydroxyl, carbonyl, and ether groups on graphene not only opens up the band gap, but also provides an option to tune the electronic, optical, and mechanical properties by means of controlled oxidation.[10] On the other hand, reduction of GO gives the possibility for the mass production of graphene.[11−17]

Although GO was discovered in the 19th century, its structure and chemical compositions are still under debate.[18,19] Various chemical compositions of GO were proposed in the last two decades, which suggests different compositions of carbon, oxygen, and hydrogen.[20−26] However, on the basis of all the suggested compositions of GO, it is clear that GO possesses oxygen mainly in the form of hydroxyl and epoxy groups, with a very small contribution of carbonyl and carboxyl groups, which predominantly decorate the edges of the graphene sheets. Apparently, all the chemical formulas of GO obtained experimentally describe 25%−75% coverage of graphene; that is, there is a combination of sp^2 and sp^3 hybridizations present in GO.[17,27,28] The sp^2 hybridization is due to the carbon atoms which are either bonded to neighboring carbon atoms (which are not connected with hydroxy or epoxy groups) or when they are bonded with oxygen in the form of carbonyl or carboxyl groups, whereas sp^3 hybridization emerges due to bonding of a carbon atom with epoxy and/or hydroxyl groups. The combination of sp^2 and sp^3 bonded carbon atoms together with the defects, breaks the symmetry of graphene and opens up a band gap, thereby, making GO a promising candidate for the opto-electronic industry.

Chhowalla and his co-workers[10] illustrated a blue shift in the EELS spectrum of GO with respect to pristine graphene using a GO sheet with around 40% of sp^3 hybridization. Moreover, in an another paper they demonstrated that by means of controlled reduction of originally synthesized GO, the

* Address correspondence to Priya_Johari@brown.edu, Vivek_Shenoy@brown.edu.

Received for review July 19, 2011 and accepted August 29, 2011.

Published online August 29, 2011
10.1021/nn202732t

© 2011 American Chemical Society

TABLE 1. *k*-Points Mesh Used for the Relaxation and the Electronic Structure Calculations (vac ≈ 12 Å) and for the Loss Spectra Calculations (vac ≈ 27 Å), for Graphene (Gr) and Graphene Oxide (GO) with Various Configurations and Functional Groups Depicted in Figure 4. The Number of Atoms in the Unit Cell and Formation Energies of the Systems Presented in Figure 4 Are Also Mentioned

			functional groups			*k* mesh		
structure	no. of atoms in the unit cell	sp^3 bonded carbon atoms (%)	epoxy	hydroxyl	carbonyl	vac ≈ 12 Å	vac ≈ 27 Å	E_{form} (eV)
Gr	4	0	0	0	0	45 × 45 × 1	45 × 45 × 1	-
a	9	25	1	0	0	35 × 25 × 1	25 × 15 × 1	0.13
b	10	50	2	0	0	35 × 25 × 1	25 × 15 × 1	0.08
c	10	50	2	0	0	35 × 25 × 1	25 × 15 × 1	−0.16
d	11	75	3	0	0	35 × 25 × 1	25 × 15 × 1	−1.09
e	11	75	3	0	0	35 × 25 × 1	25 × 15 × 1	−0.82
f	6	100	2	0	0	45 × 45 × 1	20 × 40 × 1	−0.94
g	6	100	2	0	0	45 × 45 × 1	20 × 40 × 1	−0.76
h	13	50	1	2	0	35 × 25 × 1	25 × 15 × 1	−3.53
i	14	75	2	2	0	35 × 25 × 1	25 × 15 × 1	−4.67
j	42	50	2	8	0	8 × 32 × 1	8 × 32 × 1	−17.04
k	24	100	4	4	0	21 × 42 × 1	10 × 20 × 1	−11.17
l	10	0	0	0	2	35 × 25 × 1	25 × 15 × 1	−0.47
m	16	0	0	0	4	30 × 15 × 1	20 × 10 × 1	−2.24
n	22	0	0	0	6	30 × 15 × 1	12 × 8x1	−4.09

electronic and optical properties of GO can be tuned and it can be transformed from an insulator to an electronically and optically active material.[29] While they indicated the variation in the size, shape, and relative fraction of the sp^2-hybridized domains of GO responsible for the change in properties, it is also essential to identify and understand the role of the individual functional groups in order to interpret its opto-electronic properties. Experimentally it is difficult to analyze the role of a particular functional group in describing the properties of a material that contains a bunch of functional groups. Theoretically, Boukhvalov *et al.*[28] and Lahaye *et al.*[30] modeled graphite oxide, while Yan *et al.*[9] set up GO considering various positions and coverages of epoxy and hydroxyl groups to investigate the evolution of the electronic structure with respect to various concentrations of the functional groups. However, as per our knowledge, none of the previous calculations considered the impact of a particular functional group and its concentration on the optical properties of GO. Moreover, most of the theoretical models considered GO composed of epoxides (−O−), hydroxyls (−OH), and a combination of both, while the effect of carbonyls was hardly analyzed. In carbonyls (−C═O), oxygen is attached to carbon *via* sp^2 bonding. They are demonstrated as the stable functional groups, which are hard to deoxidize,[17] and thus, they can play an important role in determining the opto-electronic properties of the reduced GO. We, therefore, in this paper present an *ab initio* density functional theory based study of the linear optical properties of GO with different coverages and compositions. To this extent, we examined the electron energy loss spectrum (EELS) of several models of GO, exhibiting various concentrations of epoxides, epoxides+hydroxyls, and carbonyls.

RESULTS AND DISCUSSION

The formation energies calculated using eq 1 for various coverages and compositions of GO are presented in Table 1. It is evident from Table 1 that except for structures a and b, all configurations are stable. The unstability of structure with 25% concentration of epoxides (see Figure 4a) is in ageement with the results of Boukhvalov *et al.*[28] We see that in 50% coverage (see Figure 4b,c), a structure having epoxides at the armchair site of the hexagonal ring is unstable, but the configuration with epoxides at the zigzag site is energetically favorable. The epoxides in Figure 4b pull the carbon atoms coupled to them in the opposite direction of the graphene sheet, and thus cause widening of graphene basal plane in the *z*-direction, which makes it an unstable structure. This widening gets minimized and the structure becomes stable when one of the epoxy lies on the side of other epoxy on opposite side of the basal plane (see Figure 4c). This is further confirmed from Figure 4d,e, which exhibit 75% coverage. We find that structure d is energetically more favorable than structure e (see Table 1). In structure d, the epoxy functional group lying adjacent to the other two epoxides faces opposite to them and thus minimizes the stretching of the graphene basal plane in the perpendicular direction and makes the configuration relatively favorable. This spliting reduces further with 100% coverage (see Figure 4f,g), where the stretching by epoxides at one side is balanced by the epoxides on the other side. However, we find that configurations with 100% coverage of epoxides are less stable than

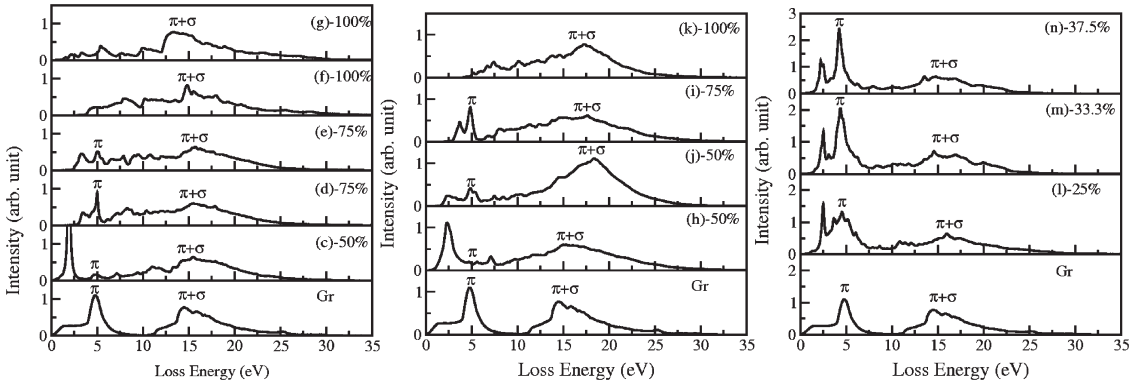

Figure 1. Electron energy loss spectra (EELS) of graphene oxide with epoxy (left), epoxy and hydroxyl (center), and carbonyl (right) functional groups, when q∥a. The naming convection of each individual spectrum corresponds to the respective structure presented in Figure 4. For direct comparison, the EELS of pristine graphene (Gr) is also given.

the structures with 75% (see Table 1), which is in agreement with previous results.[9,31]

On examining the formation energies of model structures of GO exhibiting both epoxy and hydroxyl functional groups ((see Figure 4h−k), we find that these structures are energetically more favorable than the epoxide-only phases (see Table 1). This is in agreement with the experiments which show epoxides and hydroxyls to be the major functional groups in GO.[25,32] The formation energies decrease with the increase in the concentration of epoxy and hydroxyl functional groups. However, our results replicate the previous findings[9] by demonstrating the structure with stripes of pristine and oxidized graphene at 50% coverage, to be the most favorable among all the models studied (see Figure 4j)

Structures l, m, and n which exhibit 2, 4, and 6 carbonyl groups, respectively, are also found to be stable (see Table 1). The formation energy decreases with the increase in carbonyl groups at the adjacent sites. We see from Table 1 that just by adding one carbonyl pair, the energy reduces to approximately 1.8 eV. The increase in the carbonyl groups, raises the width of the hole which leads to the cutting of the GO sheet[33] and results in a decrease in energy.

The major aim of the current work is to analyze the role of individual functional group in the EELS spectrum of GO. We, therefore, calculate EELS for model structures with varying coverages and compositions. Figure 1 depicts the calculated EELS for all the stable structures presented in Figure 4. The left panel of Figure 1 presents EELS for GO containing only epoxy functional groups, the central panel corresponds to the loss spectra of GO with epoxy and hydroxyl groups, while the right-most graphs show the results for GO exhibiting only carbonyl groups. These spectra are computed using the imaginary part of the inverse of frequency dependent dielectric constant, $\mathrm{Im}(\varepsilon^{-1}_{\alpha\beta}(\omega))$, when the scattering vector **q** is parallel to the basal plane (**q**∥**a**). For the sake of comparison, we also calculate EELS of pristine graphene (Gr). It is clear from the loss spectrum of graphene (Gr) that the π and $\pi+\sigma$ plasmon peaks appear at around 4.8 and 14.5 eV (see bottom-most graphs presented in Figure 1), which is in excellent agreement with the results of Geim and co-workers.[34,35] On examining the loss spectra of graphene covered with epoxides (see left panel of Figure 1), we find that with the increase in coverage up to 75%, the $\pi+\sigma$ plasmon peak spreads over a wide energy range and even shifts toward higher energies by roughly 1.0 eV compared to that of graphene, while the π peak is found to be less affected by the increase in concentration of epoxides. On examining the central panel of Figure 1, we discover that the blue shift of $\pi+\sigma$ plasmon peak is even more significant when both eopxy and hydroxyl groups are present. By varying the concentration of epoxy and hydroxyl functional groups, one can vary the position of the $\pi+\sigma$ plasmon peak over a wide energy range of about 0.5−3.0 eV and thus, can tune the dielectric and optical properties of GO with the means of controlled deoxidation. The π plasmon peak, however, again seems to be less sensitive to the coverage and lies between 4.8−5.2 eV when the coverage is 25%−75%. In the case of 100% coverage, that is, on complete oxidation of graphene, the π plasmon peak diminishes, as all the carbon atoms in GO become sp^3 bonded. On comparing the EELS of two structures with 50% coverage of graphene by epoxides and hydroxyls (see Figure 4h,j) we find that the π plasmon peak of graphene at around 4.8 eV is clearly visible for the structure j of GO, which carries stripes of pristine and oxidized graphene. On comparing the $\pi+\sigma$ plasmon peak in the EELS of structures h and j with respect to the $\pi+\sigma$ plasmon peak of graphene (Gr), we find a considerable blue shift of about 3 eV in case of structure j, while the feature shifts only by 0.5 eV in case of structure h. Our results for the most stable model structure j are found to be in very good agreement with the experimental results of Chhowalla and his co-workers,[10] who measured the π and $\pi+\sigma$ plasmon peaks of 40% covered GO at 5 and 19 eV, respectively. A direct comparison however cannot be made as our modeled configuration is not similar

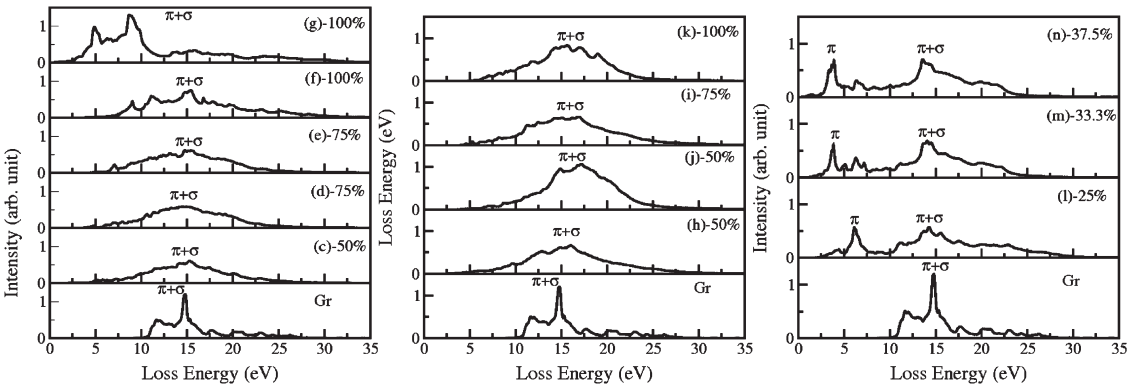

Figure 2. Electron energy loss spectra (EELS) of graphene oxide with epoxy (left), epoxy and hydroxyl (center), and carbonyl (right) functional groups, when q∥c. The naming convention for each individual spectrum corresponds to the respective structure presented in Figure 4. For direct comparison the EELS of pristine graphene (Gr) is also given.

to the configuration of GO used in the measurements. Our results, however, mainly present the trends and elucidate that the GO structure is majorly a combination of covered and uncovered stripes of graphene and 50% of coverage by epoxy and hydroxyl groups can cause a blue shift of roughly 3−4 eV in the $\pi + \sigma$ peak of GO, as compared to graphene.

On analyzing the model structures of GO which exhibit only sp^2 bonded carbon atoms, that is, when oxygen is available in the form of carbonyl groups, we find the loss peak corresponding to π plasmon to be red-shifted as compared to that of pure graphene, with the increase in oxygen-to-carbon ratio, while the feature corresponding to the $\pi + \sigma$ plasmon remains almost unaffected and lies at around 15 eV (see right panel of Figure 1). Compared to that of graphene, the π plasmon shifts toward lower energy by approximately 1 eV when the O:C ratio is 37.5%. Thus, the π plasmon excitation can be modulated by varying the size of the hole, that is, by changing the concentration of consecutive carbonyl groups. Hence, our results illustrate that in GO, the carbonyl groups are mainly responsible for shifting the π plasmon peak of the loss spectra toward the low energy region, while epoxides and hydroxyls mainly control the high energy part of the loss spectra. As in unreduced GO, oxygen is mainly present in the form of epoxy and hydroxyl groups, while a very small amount of carbonyls is present, the EELS spectra is found to be blue-shifted as compared to that of graphene.[10] Our results also support the experimental results of Eda *et al.*,[36] who demonstrated a prominent feature corresponding to π−π* transition at around 4.5−5.5 eV in the optical absorption spectrum of GO. This feature also exhibits a shoulder at 4.1 eV, which corresponds to the transition due to carbonyl groups.[27,36] On the basis of our results, we predict that a reduced GO which mainly contains thermondynamically stable carbonyl groups could be a good source for obtaining photoluminescense in the infrared and visible regions. Moreover, our study shows that EELS could be a useful tool in determining the coverage and composition of the reduced GO by analyzing the signature characteristic of a particular functional group/s, dicussed in the present work.

We also studied EELS for all the stable model structures when the scattering vector **q** is perpendicular to the basal plane, that is, when **q**∥**c** (note that lattice vectors **a** and **b** lie parallel to basal plane, while **c** lies perpendicular to it). For pure graphene, as in refs 34 and 35, we obtain no energy loss up to 11 eV and beyond that, two peaks are found roughly at 12 and 14.8 eV. The left, central, and right panels of Figure 2 present the respective EELS for GO with epoxides, epoxides+hydroxyls, and carbonyls. It is evident from the plots that in the case of epoxides and epoxides+hydroxyls, even at low coverages, the spectra exhibit mainly one peak which is smeared over a wide energy range between 5 and 25 eV. Like the loss spectra corresponding to **q**∥**a**, no shift in the $\pi + \sigma$ plasmon peak is noticed. However, in EELS of GO having carbonyl groups, a red shift in the spectra with the increase in the O:C ratio and an additional feature at lower energy side of the spectra is observed. This π plasmon feature is found at around 6 eV when the O:C ratio is 25%, which shifts toward the lower energy with the increase in the O:C ratio. We attribute the origin of this π plasmon feature to the out-of-plane stretching of sp^2 bonded carbon atoms attached to the oxygen atoms. These results again demonstrate that reduced GO with carbonyl functional groups could exhibit photoluminescence.

To further support our findings we next analyze the dependence of the optical gap on the concentration of various functional groups. Note that in the current work the optical gap is not the band gap but the lowest π−π* gap as obtained in the density of states graph. In molecules, however, the band gap and the optical gap are same as they exhibit flat bands, but in case of 2D graphene which exhibit oscillating bands, the band gap is zero while the optical gap is found to be 4 eV (see left panel of Figure 3). A peak corresponding to this lowest π−π* gap actually appears in the

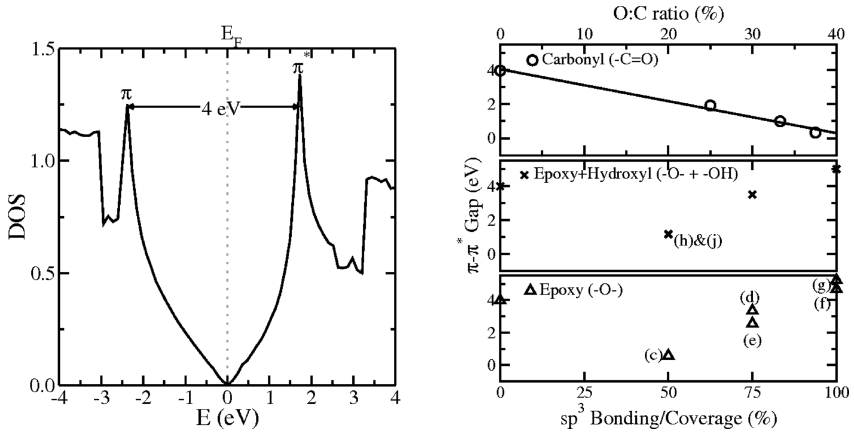

Figure 3. (Left) DOS of pristine graphene, showing the optical gap, *i.e.*, the $\pi-\pi^*$ gap to be 4 eV. Dotted line depicts the Fermi level. (Right) Optical gap of various compositions of graphene oxide with respect to its coverage by the functional groups. The optical gap is plotted with respect to the percentage of sp^3 bonded carbon atoms (coverage) for epoxides and hydroxyls (lower and middle plots), while for GO with carbonyl groups, it is plotted with respect to the O:C ratio (upper plot). Solid line shows the linear fit.

spectrum of the imaginary part of the frequency-dependent dielectric tensor (which represents the linear optical absorption), if the lowest band-to-band transition is dipole-allowed for that particular system.[37] Since, our calculations are done within the independent-particle approximation, that is, ignoring electron−hole interactions in the excitation process, a more sophisticated calculation based on the Bathe−Salpter equation would be needed to account for the excitonic effects and calculate the true optical gap. This is, however, outside the scope of present work. Moreover, it is well-known that the GGA-PBE exchange-correlation functional underestimates the excited state properties. The use of hybrid functionals is however difficult for such a large and ambitious computational study. Nevertheless, we expect that, though our calculated optical gaps are not exact, the excitonic optical gap will follow the same trends as shown in the right panel of Figure 3, which presents the $\pi-\pi^*$ gap for various coverages (O:C ratio) of GO by epoxides and hydroxyls (carbonyls). On analyzing the plots corresponding to the case of epoxides and epoxides+hydroxyls we find that the optical gap of pristine and fully oxidized graphene is larger than that of the reduced GO. The optical gap is found to be a minimum for the case of 50% coverage. While, in case of carbonyl groups, the optical gap decreases linearly with the increase in oxygen-to-carbon ratio. The optical gap reduces from 4.0 to 0.3 eV when the O:C ratio changes from 0% to 37.5%. However, before arguing that reduced GO with cabonyls as the prominent functional group could be useful in realizing graphene-based opto-electronic devices, we calculate the band gap of the model configurations presented in Figure 4l,m,n. We find zero band gap for GO with 25% of O:C ratio. However, the band opens up and increases linearly with the increase in the concentration of carbonyl groups. For 33.3%, and 37.5% of O:C ratio, we obtain a band gap of 0.05 and 0.12 eV, respectively. Note that the presented

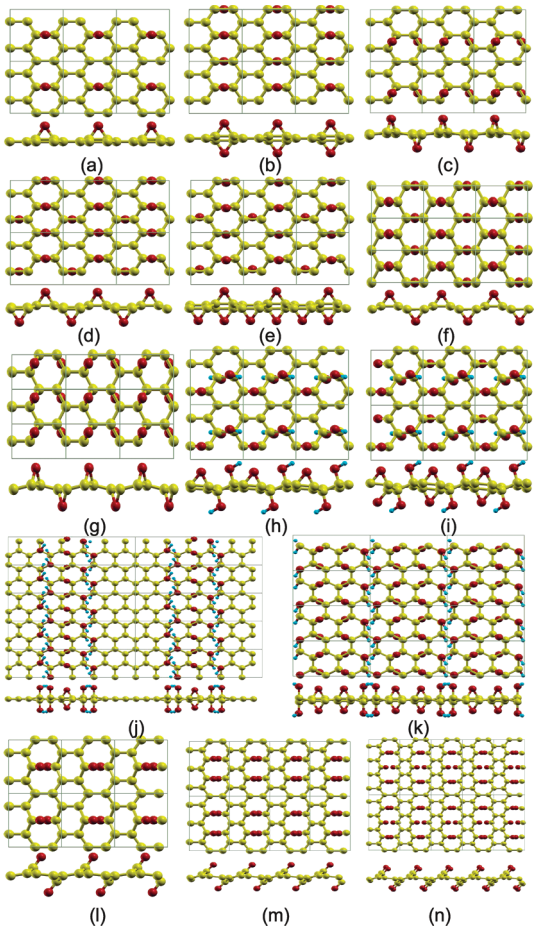

Figure 4. Top and side view of the various configurations of graphene oxide. GO with various coverages of epoxy functional groups are depicted: (a) 25%, (b, c) 50%, (d, e) 75%, and (f, g) 100%. Configurations h, i, j, and k represent 50%, 75%, 50%, and 100%, respectively, coverage of the graphene basal plane by epoxy and hydroxyl functional groups. GO with carbonyl groups are shown in configurations l, m, and n with two, four, and six carbonyl groups, respectively.

values are band gaps (Kohn−Sham gaps) with the PBE exchange correlation functional, which are well-known

to be underestimated.[38] We see that the band gap increases while the optical gap decreases and at some point they should be equal. This shows that with the increase in the length of the hole, bands become flatter and orbitals become localized, which shows a signature of oxygen-terminated zigzag graphene nanoribbons.[4,38−40] Our results agree with the experimental findings, which demonstrated the thermally and chemically reduced GO to be electrically and optically active.[27,29,36,41,42]

CONCLUSIONS AND FUTURE DIRECTIONS

In this work we have performed DFT-based calculations to study the individual role of major functional groups present in graphene oxide, in determining its electronic and optical properties. In agreement with experiments, our calculations demonstrate a blue shift in the EELS spectra when GO is 25%−75% covered with epoxides and hydroxyls. For the corresponding model structures condsidered in the present work, the $\pi + \sigma$ plasmon peak shifts by roughly 1.0−3.0 eV, while a blue shift of around 0.4 eV is obtained for the π plasmon, when $\mathbf{q} \| \mathbf{a}$. Our results predict a red shift in the EELS spectrum when oxygen in GO is present mainly in the form of carbonyl groups. The π plasmon feature is found at approximately 4.0 eV, as compared to 4.8 eV in graphene, when the oxygen-to-carbon ratio is 37.5% in GO exhibiting only carbonyl groups. Our results also reveal that unlike EELS of graphene, which does not possess any feature until 11 eV when $\mathbf{q} \| \mathbf{c}$, GO manifests a broad $\pi + \sigma$ peak lying between 5−25 eV. In the case of carbonyl groups, this broad feature is even coupled with a π plasmon peak in the low energy region of the loss spectra, which makes the configuration favorable for photoluminescense. Moreover, we have shown that the optical gap of reduced graphene oxides is lower than the optical gap of pristine and fully oxidized graphene sheets (4 eV). We also demonstrated that the increase in the size of the hole or defect in the case of carbonyl groups, decreases the optical gap rapidly and show a reduction in optical gap from 4.0 to 0.3 eV when oxygen-to-carbon ratio changes from 0% to 37.5%. Thus, through our EELS and optical gap calculations for various model structures, we demonstrated the significance of the concentration of various functional groups in modulating the optical properties of GO and also supported the experimental results, which proposed the tunning of the electronic and optical properties of reduced graphene oxide *via* controlled deoxidation. In the current work, we considered periodic structures, whereas all fabricated structures are mainly amorphous. Therefore, in the future we would like to study amorphous GO to examine the influence of disordered GO on optical properties.

STRUCTURAL MODELS

To analyze the evolution of the optical properties of GO with the change in concentration of various functional groups, we model GO with different coverages of epoxides, epoxides and hydroxyls, and carbonyls. Figure 4 depicts the various compositions of GO considered in the present work. Most of the model structures are chosen from the previously proposed structures by Boukhvalov *et al.*[28] and Yan *et al.*[9] To model GO with various concentration of epoxides, we consider 25%−100% coverage of the graphene basal plane and different positions of the functional group (see Figure Figure 4a−g). For example, we study two structures for the 50% coverage of graphene (see Figure 4b,c) by considering a unit cell with eight carbon atoms, in which four carbon atoms are bonded with the epoxy functional group *via* sp^3 bonding, while the other four share a bond with carbon atoms and possess sp^2 type of bonding. In the structure depicted in Figure 4 b, oxygen atoms (one on the upper side and the other on the lower side of the basal plane) are arranged between the carbon atoms at the armchair site, while in the other structure (see Figure 4 c) they lie in between the carbon atoms forming a zigzag chain. Similar kind of arrangements are also considered for the 100% coverage of the graphene basal plane (see Figure 4f,g). In the case of 75% coverage, one structure possesses epoxides attached to the same ring, on the same side of the basal plane (see Figure 4d), while they oppose each other in the other structure (see Figure 4e).

The nuclear magnetic resonance (NMR) results of Ruoff *et al.*[25] demonstrated the presence of a large fraction of carbon atoms bonded to epoxides and hydroxyls in the sheets of graphite oxide. Boukhvalov *et al.*[28] and Yan *et al.*[9] also found the structures having both epoxides and hydroxyls to be energetically more favorable than the configurations with only epoxide or hydroxyl function groups. Therefore, we also calculate EELS for different combinations of epoxides and hydroxyls with 50%, 75%, and 100% coverage of the graphene basal plane. For 50% coverage, we analyze two structures (see Figure 4h,j). In one structure (see Figure 4h) we consider a small unit cell with eight carbon atoms, one epoxide, and two hydroxyl groups, while in the other structure (see Figure 4j) we choose a large unit cell with 24 carbon atoms, 2 epoxides, and 8 hydroxyls. Epoxides are arranged at the armchair site of the carbon ring in the first structure, while in the latter structure, they lie at the zigzag site. Moreover, in structure j, there are separate clusters of sp^2 and sp^3 bonded carbon atoms. Yan *et al.*[9] found this structure to be the most favorable among the other structures studied by them. The 75% coverage of GO with epoxy and hydroxyl functional groups is modeled using eight carbon atoms with two epoxides and two hydroxyls, lying on both sides of the basal plane (see Figure 4i). To examine 100% coverage (see Figure 4k), we consider the model proposed by Yan *et al.*[9] for the fully oxidized graphene, which possesses 12 carbon atoms with four epoxides and four hydroxyls in the unit cell.

The carbonyl group, which decorates the edges of GO, is mainly found in pairs.[17,33] Bagri *et al.*[17] demonstrated carbonyls to be one of the most stable functional groups, which are hard to reduce without destroying the graphene basal plane. Li *et al.*[33] also showed a carbonyl pair to be more stable than an epoxy pair. They suggested a reaction pathway for the conversion of the epoxy pair to the carbonyl pair, which governs the cutting of the GO sheet. The oxygen atoms in the pair of carbonyl groups are arranged opposite to each other on both sides of the basal plane and create a hole between the carbon atoms to which they are attached. The increase in carbonyl pairs at consecutive sites increases the size of the hole, and thereby, affects the properties of GO. To study the effect of the width of the hole, we studied GO with two, four, and six carbonyl groups corresponding to the O:C ratio of 25%, 33.3%, and 37.5%, respectively (see Figure 4l−n).

COMPUTATIONAL DETAILS

First principles density functional theory (DFT) based calculations were performed to study the impact of concentration of various functional groups in GO (see Figure 4) using the Vienna ab initio simulation package (VASP).[43,44] Projector-augmented-wave (PAW) potentials[45] were used to mimic the ionic cores, while the generalized gradient approximation (GGA) in the Perdew–Burke–Ernzerhof[46] (PBE) model was employed for the exchange and correlation functional. All the structures depicted in Figure 4 were relaxed until the atomic forces were smaller than 0.01 eV/Å. In the relaxation simulations, along with the atomic coordinates, we also allowed variation of the cell dimensions. We used a periodic simulation cell with around a 12 Å thick vacuum region in the direction normal to the graphene sheet for the cell relaxation and the electronic structure calculations. However, a large vacuum thickness is required for the loss spectra calculations, therefore, we used a vacuum of 27 Å for the study of plasmons. Calculations were performed using the plane wave cutoff of 600 eV. Since the model structures exhibit different unit cells, *k*-points were chosen accordingly. The *k*-point mesh used for the calculations of various model structures are tabulated in the Table 1.

To examine the stability of the structures discussed in the present work we calculated formation energy using following formula:

$$E_{\text{form}} = E_{C_xO_y(OH)_z} - \frac{x}{8}E_{C_8} - \frac{y}{2}E_{O_2} - zE_{OH} \quad (1)$$

In the above formulation, $E_{OH} = E_{H_2O}/2 + E_{O_2}/4$, where E_{H_2O}, E_{O_2}, and E_{OH} are the energies of water molecule, oxygen molecule, and the hydroxyl radical, respectively. In eq 1, $E_{C_xO_y(OH)_z}$ defines the total energy of the optimized cell and E_{C_8} gives the total energy of the graphene supercell having eight atoms.

To understand the optical properties of the GO sheets, it is important to evaluate their frequency-dependent dielectric response functions such as absorption or electron energy loss spectra (EELS). We, therefore, in the current paper calculated EELS in the long-wavelength limit $q \rightarrow 0$, which essentially determines the optical properties in the wavelength regime accessible to optical or electronic probes. The loss spectra were computed by taking the imaginary part of inverse of the longitudinal expression of the frequency-dependent microscopic dielectric tensor, $\varepsilon_{\alpha\beta}$, in the random phase approximation (RPA).[47] The longitudinal expression for the imaginary part of the frequency dependent dielectric tensor is given as

$$\varepsilon^{(2)}_{\alpha\beta}(\omega) = \frac{4\pi^2e^2}{\Omega}\lim_{q\rightarrow 0}\frac{1}{q^2}\sum_{c,v,\mathbf{k}} 2w_{\mathbf{k}}\delta(\varepsilon_{c\mathbf{k}} - \varepsilon_{v\mathbf{k}} - \omega) \times\langle u_{c\mathbf{k}+e_\alpha q}|u_{v\mathbf{k}}\rangle\langle u_{c\mathbf{k}+e_\beta q}|u_{v\mathbf{k}}\rangle^* \quad (2)$$

Here the indices *c* and *v* refer to the conduction and the valence band states, respectively, **k** is the Bloch wave vector, $w_{\mathbf{k}}$ are the **k**-point weights (which are defined such that they sum to 1), the factor 2 before the weights accounts for the fact that a spin-degenerate system is considered, and Ω is the volume of the unit cell. The vectors e_α are the unit vectors for the three Cartesian directions. Note that the frequency ω has the dimensions of energy. VASP calculates the imaginary part of the frequency dependent dielectric tensor for $q = 0$ and uses the Kramers–Kronig transformation to obtain its real part.[48] The RPA approximation accounts for the weak screened Coulomb interaction to describe the dynamic linear electronic response of plasmons at the mean-field level, and thus, our calculations miss the many-body effects. However, the agreement of our previous EELS calculations[49,50] with the experimental spectra[34,49,51] convinces us as to the reliabilty of the above-mentioned approach.

Acknowledgment. The support of the Army Research Office through Contract W911NF-11-1-0171 is gratefully acknowledged. Computational support for this research was provided by Grant TG-PHY100022 and TG-DMR090098 from the TeraGrid advanced support program, and the Center for Computation and Visualization at Brown University. P.J. thanks Rassin Grantab for the useful discussion.

REFERENCES AND NOTES

1. Geim, A. K.; Novoselov, K. S. The Rise of Graphene. *Nat. Mater.* **2007**, *6*, 183–191.
2. Park, S.; Ruoff, R. S. Chemical Methods for the Production of Graphenes. *Nat. Nanotechnol.* **2009**, *4*, 217–224.
3. Novoselov, K. S.; Geim, A. K.; Morozov, S. V.; Jiang, D.; Zhang, Y.; Dubonos, S. V.; Grigorieva, I. V.; Firsov, A. A. Electric Field Effect in Atomically Thin Carbon Films. *Science* **2004**, *306*, 666–669.
4. Han, M. Y.; Ozyilmaz, B.; Zhang, Y. B.; Kim, P. Energy Band-Gap Engineering of Graphene Nanoribbons. *Phys. Rev. Lett.* **2007**, *98*, 206805.
5. Li, X. L.; Wang, X. R.; Zhang, L.; Lee, S. W.; Dai, H. J. Chemically Derived, Ultrasmooth Graphene Nanoribbon Semiconductors. *Science* **2008**, *319*, 1229–1232.
6. Wu, X. S.; Sprinkle, M.; Li, X. B.; Ming, F.; Berger, C.; de Heer, W. A. Epitaxial-Graphene/Graphene-Oxide Junction: An Essential Step Towards Epitaxial Graphene Electronics. *Phys. Rev. Lett.* **2008**, *101*, 026801.
7. Jung, I.; Dikin, D. A.; Piner, R. D.; Ruoff, R. S. Tunable Electrical Conductivity of Individual Graphene Oxide Sheets Reduced at "Low" Temperatures. *Nano Lett.* **2008**, *8*, 4283–4287.
8. Elias, D. C.; Nair, R. R.; Mohiuddin, T. M. G.; Morozov, S. V.; Blake, P.; Halsall, M. P.; Ferrari, A. C.; Boukhvalov, D. W.; Katsnelson, M. I.; Geim, A. K. ; *et al.* Control of Graphene's Properties by Reversible Hydrogenation: Evidence for Graphane. *Science* **2009**, *323*, 610–613.
9. Yan, J. A.; Xian, L. D.; Chou, M. Y. Structural and Electronic Properties of Oxidized Graphene. *Phys. Rev. Lett.* **2009**, *103*, 086802.
10. Mkhoyan, K. A.; Contryman, A. W.; Silcox, J.; Stewart, D. A.; Eda, G.; Mattevi, C.; Miller, S.; Chhowalla, M. Atomic and Electronic Structure of Graphene-Oxide. *Nano Lett.* **2009**, *9*, 1058–1063.
11. Schniepp, H. C.; Li, J. L.; McAllister, M. J.; Sai, H.; Alonso, M. H.; Adamson, D. H.; Prudhomme, R. K.; Car, R.; Saville, D. A.; Aksay, I. A. Functionalized Single Graphene Sheets Derived from Splitting Graphite Oxide. *J. Phys. Chem. B* **2006**, *110*, 8535–8539.
12. Stankovich, S.; Dikin, D. A.; Piner, R. D.; Kohlhaas, K. A.; Kleinhammes, A.; Jia, Y.; Wu, Y.; Nguyen, S. T.; Ruoff, R. S. Synthesis of Graphene-Based Nanosheets *via* Chemical Reduction of Exfoliated Graphite Oxide. *Carbon* **2007**, *45*, 1558–1565.
13. Gilje, S.; Han, S.; Wang, M.; Wang, K. L.; Kaner, R. B. A Chemical Route to Graphene for Device Applications. *Nano Lett.* **2007**, *7*, 3394–3398.
14. Li, D.; Mueller, M. B.; Gilje, S.; Kaner, R. B.; G., W. G. Processable Aqueous Dispersions of Graphene Nanosheets. *Nat. Nanotechnol.* **2008**, *3*, 101–105.
15. Eda, G.; Fanchini, G.; Chhowalla, M. Large-Area Ultrathin Films of Reduced Graphene Oxide as a Transparent and Flexible Electronic Material. *Nat. Nanotechnol.* **2008**, *3*, 270–274.
16. Gomez-Navarro, C.; Weitz, R. T.; Bittner, A. M.; Scolari, M.; Mews, A.; Burghard, M.; Kern, K. Electronic Transport Properties of Individual Chemically Reduced Graphene Oxide Sheets. *Nano Lett.* **2007**, *7*, 3499–3503.
17. Bagri, A.; Mattevi, C.; Acik, M.; Chabal, Y. J.; Chhowalla, M.; Shenoy, V. B. Structural Evolution during the Reduction of Chemically Derived Graphene Oxide. *Nat. Chem.* **2010**, *2*, 581–587.
18. Brodie, B. C. Sur le Poids Atomique du Graphite. *Ann. Chim. Phys.* **1860**, *59*, 466–472.
19. Staudenmaier, L. Verfahren zur Darstellung der Graphitsaeure. *Ber. Dtsch. Chem. Ges.* **1898**, *31*, 1481–1487.
20. Nakajima, T.; Mabuchi, A.; Hagiwara, R. A New Structure Model of Graphite Oxide. *Carbon* **1988**, *26*, 357–361.
21. Szabo, T.; Tombacz, E.; Illes, E.; Dekany, I. Enhanced Acidity and pH-Dependent Surface Charge Characterization of Successively Oxidized Graphite Oxides. *Carbon* **2006**, *44*, 537–545.
22. Hontora-Lucas, C.; Lopez-Peinado, A. J.; Lopez-Gonzalez, J. d. D.; Rojas-Cervantes, M. L.; Martin-Aranda, R. M. Study of Oxygen-Containing Groups in a Series of Graphite

Oxides: Physical and Chemical Characterization. *Carbon* **1995**, *33*, 1585–1592.
23. Stankovich, S.; Piner, R. D.; Nguyen, S. T.; Ruoff, R. S. Synthesis and Exfoliation of Isocyanate-Treated Graphene Oxide Nanoplatelets. *Carbon* **2006**, *44*, 3342–3347.
24. Cassagneau, T.; Guerin, F.; Fendler, J. H. Preparation and Characterization of Ultrathin Films Layer-by-Layer Self-Assembled from Graphite Oxide Nanoplatelets and Polymers. *Langmuir* **2000**, *16*, 7318–7324.
25. Cai, W. W.; Piner, R. D.; Stadermann, F. J.; Park, S.; Shaibat, M. A.; Ishii, Y.; Yang, D. X.; Velamakanni, A.; An, S. J.; Stoller, M.; *et al.* Synthesis and Solid-State NMR Structural Characterization of C-13-Labeled Graphite Oxide. *Science* **2008**, *321*, 1815–1817.
26. Lu, N.; Huang, Y.; Li, H. B.; Li, Z. Y.; Yang, J. L. First Principles Nuclear Magnetic Resonance Signatures of Graphene Oxide. *J. Chem. Phys.* **2010**, *133*.
27. Eda, G.; Lin, Y. Y.; Mattevi, C.; Yamaguchi, H.; Chen, H. A.; Chen, I. S.; Chen, C. W.; Chhowalla, M. Blue Photoluminescence from Chemically Derived Graphene Oxide. *Adv. Mater.* **2010**, *22*, 505–509.
28. Boukhvalov, D. W.; Katsnelson, M. I. Modeling of Graphite Oxide. *J. Am. Chem. Soc.* **2008**, *130*, 10697–10701.
29. Loh, K. P.; Bao, Q. L.; Eda, G.; Chhowalla, M. Graphene Oxide as a Chemically Tunable Platform for Optical Applications. *Nat. Chem.* **2010**, *2*, 1015–1024.
30. Lahaye, R.; Jeong, H. K.; Park, C. Y.; Lee, Y. H. Density Functional Theory Study of Graphite Oxide for Different Oxidation Levels. *Phys. Rev. B* **2009**, *79*, 125435.
31. Li, J. L.; Kudin, K. N.; McAllister, M. J.; Prud'homme, R. K.; Aksay, I. A.; Car, R. Oxygen-Driven Unzipping of Graphitic Materials. *Phys. Rev. Lett.* **2006**, *96*, 176101.
32. Lerf, A.; He, H. Y.; Forster, M.; Klinowski, J. Structure of Graphite Oxide Revisited. *J. Phys. Chem. B* **1998**, *102*, 4477–4482.
33. Li, Z. Y.; Zhang, W. H.; Luo, Y.; Yang, J. L.; Hou, J. G. How Graphene Is Cut upon Oxidation? *J. Am. Chem. Soc.* **2009**, *131*, 6320.
34. Eberlein, T.; Bangert, U.; Nair, R. R.; Jones, R.; Gass, M.; Bleloch, A. L.; Novoselov, K. S.; Geim, A.; Briddon, P. R. Plasmon Spectroscopy of Free-Standing Graphene Films. *Phys. Rev. B* **2008**, *77*, 233406.
35. Gass, M. H.; Bangert, U.; Bleloch, A. L.; Wang, P.; Nair, R. R.; Geim, A. K. Free-Standing Graphene at Atomic Resolution. *Nat. Nanotechnol.* **2008**, *3*, 676–681.
36. Eda, G.; Chhowalla, M. Chemically Derived Graphene Oxide: Towards Large-Area Thin-Film Electronics and Optoelectronics. *Adv. Mater.* **2010**, *22*, 2392–2415.
37. Sony, P.; Shukla, A.; Ambrosch-Draxl, C. Energetics and Electronic Structure of Phenyl-Disubstituted Polyacetylene: A First-Principles Study. *Phys. Rev. B* **2010**, *82*, 035213.
38. Ramasubramaniam, A. Electronic Structure of Oxygen-Terminated Zigzag Graphene Nanoribbons: A Hybrid Density Functional Theory Study. *Phys. Rev. B* **2010**, *81*, 245413.
39. Barone, V.; Hod, O.; Scuseria, G. E. Electronic Structure and Stability of Semiconducting Graphene Nanoribbons. *Nano Lett.* **2006**, *6*, 2748–2754.
40. Tapaszto, L.; Dobrik, G.; Lambin, P.; Biro, L. P. Tailoring the Atomic Structure of Graphene Nanoribbons by Scanning Tunnelling Microscope Lithography. *Nat. Nanotechnol.* **2008**, *3*, 397–401.
41. Acik, M.; Lee, G.; Mattevi, C.; Chhowalla, M.; Cho, K.; Chabal, Y. J. Unusual Infrared-Absorption Mechanism in Thermally Reduced Graphene Oxide. *Nat. Mater.* **2010**, *9*, 840–845.
42. Robinson, J. T.; Perkins, F. K.; Snow, E. S.; Wei, Z. Q.; Sheehan, P. E. Reduced Graphene Oxide Molecular Sensors. *Nano Lett.* **2008**, *8*, 3137–3140.
43. Kresse, G.; Furthmuller, J. Efficient Iterative Schemes for *ab Initio* Total-Energy Calculations Using a Plane-Wave Basis Set. *Phys. Rev. B* **1996**, *54*, 11169–11186.
44. Kresse, G.; Furthmuller, J. Efficiency of *ab Initio* Total Energy Calculations for Metals and Semiconductors Using a Plane-Wave Basis Set. *Comput. Mater. Sci.* **1996**, *6*, 15–50.
45. Kresse, G.; Joubert, D. From Ultrasoft Pseudopotentials to the Projector Augmented-Wave Method. *Phys. Rev. B* **1999**, *59*, 1758–1775.
46. Perdew, J. P.; Burke, K.; Ernzerhof, M. Generalized Gradient Approximation Made Simple. *Phys. Rev. Lett.* **1996**, *77*, 3865–3868.
47. Ehrenreich, H.; Cohen, M. H. Self-Consistent Field Approach to the Many-Electron Problem. *Phys. Rev.* **1959**, *115*, 786–790.
48. Gajdos, M.; Hummer, K.; Kresse, G.; Furthmuller, J.; Bechstedt, F. Linear Optical Properties in the Projector-Augmented Wave Methodology. *Phys. Rev. B* **2006**, *73*, 045112.
49. Sun, J. B.; Hannon, J. B.; Tromp, R. M.; Johari, P.; Bol, A. A.; Shenoy, V. B.; Pohl, K. Spatially-Resolved Structure and Electronic Properties of Graphene on Polycrystalline Ni. *ACS Nano* **2010**, *4*, 7073–7077.
50. Johari, P.; Shenoy, V. B. Tunable Dielectric Properties of Transition Metal Dichalcogenides. *ACS Nano* **2011**, *5*, 5903–5908.
51. Coleman, J. N.; Lotya, M.; O'Neill, A.; Bergin, S. D.; King, P. J.; Khan, U.; Young, K.; Gaucher, A.; De, S.; Smith, R. J. ; *et al.* Two-Dimensional Nanosheets Produced by Liquid Exfoliation of Layered Materials. *Science* **2011**, *331*, 568–571.